STUDY OF FREE CONVECTION IN BINARY SYSTEMS WITH PHASE CHANGE

Tomasz A. Kowalewski
Center of Mechanic and Information Technology, IPPT PAN
Polish Academy of Sciences, PL 00-049 Warsaw
Poland

Jerzy Banaszek
Marek Rebow, Piotr Furmański and Tomasz S. Wiśniewski
Institute of Heat Engineering
Warsaw University of Technology, PL 00-665 Warsaw
Poland

ABSTRACT

The thermal convection of water and aqueous solution of sodium chloride is investigated experimentally and numerically in a cubic cavity, with two opposite vertical walls kept at prescribed temperature. The analysis is carried out for the pure convection of water in the vicinity of the freezing region (cold wall temperature T_c= 0°C), and for convection of water and its solute accompanied by freezing ($T_c \leq$ -10°C). The opposite hot wall temperature is fixed at +10°C. The time history of the velocity and temperature fields are measured using liquid crystals seeding. It was observed that the thermal boundary conditions of non-isothermal side walls have a triggering effect on the flow configuration. Investigated thermosolutal convection demonstrated transition from a double-circulation flow pattern observed for the pure water to the single, double roll circulation at the upper part of the cavity with a wide stagnant layer at the bottom.

INTRODUCTION

Properties of an alloy casting final product are, to a large degree, determined by liquid flow during a solidification process. Convective currents due to temperature and concentration gradients may produce non-homogeneous macroscopic composition of the solidified product. Unfortunately, accurate determination of the flow pattern is not simple in this case. Due to non-linearity of the governing equations, that have to be solved for both liquid and solid regions separated by a moving boundary, numerical modelling of the casting problem becomes a challenging task. Simplifications needed to overcome modelling difficulties are inherent in all numerical or analytical solutions. Their effect on the final result is usually difficult to assess, and direct comparison with physical experiments becomes very important. However, collection of the detailed experimental data is not always possible, especially for technologically interesting metal alloys. Hence, it seems necessary to verify numerical codes against experimentally simpler configurations, i.e. a well defined, simple geometry filled with a liquid which is easy to handle and describe. Motivated by such a need, we present our recent attempts to create an experimental benchmark for the solidification of both a pure liquid (water) and a binary solution (mixture of water and salt). The solidification from a vertical wall (Fig. 1) is considered as it very often occurs in practice.

Numerical modelling or experimental analysis of this complex flow scenario is not a trivial task. It requires application of full field acquisition methods, which can give transient data for velocity and temperature fields, reliable enough for their subsequent confrontation with the CFD models. Application of holographic techniques is a promising option for studding gas flow (Collins 1991), however not free from experimental complexity and data interpretation problems. In liquids, we believe that valuable alternative offers the particle image velocimetry and thermometry. It is based on application of thermochromic liquid crystals suspended in a working fluid as seeding. Digital Particle Image Velocimetry (DPIV) combined with digital colour analysis (DPIT) allow simultaneous measurement of 2-D velocity and temperature flow fields. Collected transient data for the temperature and velocity fields as well as the interface position can be directly compared with the numerical calculations.

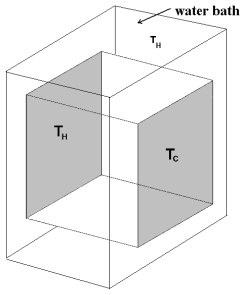

Fig. 1. The cubical box with differentially heated walls T_h - T_c. Solidification starts at the cold wall (T_c).

FORMULATION OF THE PROBLEM

We consider convective flow in a cube shaped box filled with liquid (Fig. 1). Due to the temperature difference imposed between two opposite, vertical walls natural convection develops in the cavity. Two solidification cases are investigated: freezing of pure distillate water and freezing of dilute water-sodium chloride solution. The fluid density, viscosity, thermal conductivity and heat capacity are assumed to be temperature dependent. Two opposite vertical walls are assumed isothermal. One of them is held at a temperature T_c = -15°C (or -10°C), that is below the freezing temperature of the liquid T_r, and a solid phase forms there. The opposite vertical wall is held at a temperature T_h = 10°C. The other four walls of low thermal conductivity allow the entry of heat from the external fluid which surrounds the cavity. To ensure well defined thermal boundary conditions at the side walls, the cavity is immersed in a water bath. This water bath has a constant temperature $T_{ext} = T_h$. The temperature field at the inner surfaces of the walls adjusts itself depending on both the flow inside the box and the heat flux through and along the walls.

Transient development of the flow convection and solidification is studied. Both the initial fluid temperature and the temperature of all six walls are equal to $T_o = T_h$, i.e. to the temperature of the hot wall. A zero initial velocity flow field is assumed. The convection starts when at time t=0 the cold wall temperature suddenly drops to 0°C. In the freezing experiments the selected cold wall temperatures were T_c= -15°C or -10°C.

Most of the experiments are performed for pure distillated water. Three basic dimensionless parameters defining the freezing problem driven by both conduction and free convection are the Rayleigh number (Ra), the Prandtl number (Pr) and the Stefan number (Ste), given as

$$\mathrm{Ra} = \frac{g\beta \Delta T H^3}{\alpha \nu}\ ,\quad \mathrm{Pr} = \frac{\nu}{\alpha}\ \text{ and }\ \mathrm{Ste} = \frac{c_p \Delta T}{L_f}\ ,$$

where $\Delta T = T_h - T_r$ is the difference between the temperatures of the hot wall T_h and the phase interface T_r. In the above definitions g, H, α, β, ν, c_p, L_f, denote, respectively, the gravitational acceleration, the cavity height, the thermal diffusivity, the coefficient of thermal expansion, the kinematic viscosity, the specific heat and the latent heat of fusion. The physical properties of the fluid above are taken for the arbitrary selected reference temperature T_r= 0°C. The density function and relationships for the water heat capacity, the thermal conductivity and the viscosity used are those given by Kowalewski & Rebow (1997). The thermophysical properties of ice are assumed to be constant and equal to: 916.8kg/m^3 for the density, 2.26W/mK for the thermal conductivity, and 2.116kJ/kgK for the heat capacity. The latent heat has the value of L_f = 335kJ/kg. The thermal conductivity and thermal diffusivity of the Plexiglas, of which the side walls are made, has been measured and found to be 0.195W/mK and $1.19 \cdot 10^{-7}$m^2/s, respectively. The heat transfer coefficient h, used for modelling the convective heat flux from the external fluid, is assumed to be equal to 1000W/Km^2 for the forced convection in the external water bath.

The freezing problem of the water-salt solution characterises an additional coupling of the temperature and concentration fields with the rate of propagation of the phase boundary. Initially the solution is at a uniform temperature and at a uniform concentration C_o. When the solid begins to form and move, the solute, which is rejected into the liquid, forms a region of increased concentration near the interface. The concentration gradient becomes the second force driving the flow. Two additional non-dimensional numbers appear for the concentration driven flow: a solutal Rayleigh number Ra_s based on the concentration gradient ΔC, and the Schmidt number Sc - a solutal equivalent of the Prandtl number based on the diffusivity D:

$$\mathrm{Ra}_s = \frac{g\beta_c \Delta C H^3}{D\nu}\ ,\qquad \mathrm{Sc} = \frac{\nu}{D}\ .$$

EXPERIMENTAL

Our main interest is directed to collecting quantitative information about the phase front position as well as about velocity and temperature fields within a domain of a mid-height vertical plane of the cavity. For this purpose the flow images of the centre vertical cross-section have been collected periodically every 60s or 120s, approximately during two hours from the onset of cooling. At each time step series of 3 to 10 RGB images are taken at short time interval. Later on they are used for velocity evaluation (inter images cross-correlation) and colour averaging procedures. Special acquisition and image analysis software has been developed and used to obtain 2-D flow pattern (particle tracks) and temperature and velocity fields (Abegg et al. 1994, Kowalewski & Cybulski 1996).

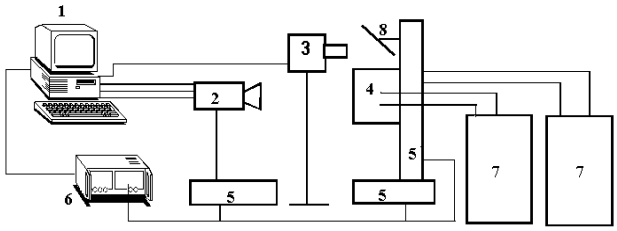

Fig. 2. Schematic of the experimental system. PC (1) with the acquisition card controlls: camera (2), halogen lamp (3) and three stepping motors (5) through driver (6). Temperature in the cavity (4) controlled by two thermostates (7). Mirror (8) used to direct light sheet.

The experimental set-up (Fig. 2) consists of a convection box, a halogen tube lamp, the 3CCD colour camera (KYF55 JVC) and the 32-bit frame grabber (IC-PCI ITI). The flow field is illuminated with a 2mm thin sheet of white light from a specially constructed halogen lamp, and observed in the perpendicular direction. The 24-bit colour images of 560x560 pixels have been acquired using a 64MB Pentium 133 computer. This set-up permits us to gain in real time over 50 images before they have to be saved on the computer magnetic disk.

The convection cubic box, of 38mm inner dimension, has two isothermal walls made of a black anodised metal. Their constant temperature is maintained by an anti-freeze coolant flowing through the attached antechamber. Four non-isothermal walls of the cavity are made of 9mm thick Plexiglas. The temperature of the cooling and heating liquids and that of the water in the bath (surrounding the four non-adiabatic walls) are controlled by thermostats. The computer controlled system of three stepping motors allows to acquire images of the several cross-sections fully automatically within several seconds. The experiment starts when the inlet valves are abruptly opened to the coolant passages. The temperatures of cold and hot walls are kept, respectively, at -15°C (-10°C) and +10°C. Distillated water and a dilute water-sodium chloride solution have been selected as flow media for their relatively well known thermophysical properties.

Liquid Crystal Thermography

As aforementioned Thermochromic Liquid Crystal (TLC) tracers (Hiller & Kowalewski 1987, Stąsiek & Collins 1989) have been applied to measure both temperature and velocity flow fields. The TLCs temperature visualisation is based on their property to reflect definite colours at specific temperatures and viewing angle. Employment of digital evaluation techniques initiated development of Digital Particle Image Velocimetry and Thermometry (Hiller et al. 1993). It allows us simultaneous and fully automatic measurements of temperature and velocity fields for selected 2-D cross-section of the flow.

Application of the DPIVT method for the freezing problem yields several additional experimental constrains. The investigated temperature range is well defined by the phase change temperature. Hence the colour-play properties of the TLC material have to be correctly matched. In addition, the ice surface generates additional light scattering and reflections. These may generate unexpected colour shifts or/and image distortions in regions adjoining the phase front, and have to be accounted for throughout the calibration procedure.

The mean diameter of the unencapsulated TLC tracers used is about 50μm. The temperature measurements are based on a digital colour analysis of *RGB* images of the TLCs seeded flow field. The incoming *RGB* signals are transformed pixel by pixel into *Hue, Saturation and Intensity*. Temperature is determined by relating the hue to a temperature calibration function (Kowalewski & Cybulski 1996), obtained from the images taken for the same fluid, at the same illumination, acquisition and evaluation conditions. Especially developed averaging, smoothing and interpolating techniques are used to remove ambiguity of resulting isotherms.

Our 8-bit representation of the hue value assures resolution better than 1%. However, the colour - temperature relationship is strongly non-linear. Hence, the accuracy of the measured temperature depends on the colour (hue) value, and varies from 3% to 10% of the full colour play range. For the TLCs used (TM from Merck) it results in the absolute accuracy of 0.15^{o}C for lower temperatures (red-green colour range) and 0.5^{o}C for higher temperatures (blue colour range). The most sensitive region is the colour transition from red to green and takes place for a temperature variation less then one Celsius degree. To improve the accuracy of temperature measurements, experiments have been repeated using four different types of TLCs, so that their combined colour play sensitivity range covered temperatures from -5^{o}C to 14^{o}C.

The colour of light refracted by TLCs depends also on the refraction angle. Our previous investigations (Hiller et al. 1988) have shown that the evaluated temperature depends linearly on the refraction angle, with the slope equal 0.07^{o}C per 10^{o} change of the angle. Therefore, it is important that the angle between illuminated plane (light sheet plane) and the camera is fixed and the observation angle of the lens is small. In the present experiment flow is observed at 90^{o} angle using 50mm lens and 1/3' sensor, i.e. the full observation angle is smaller than 4^{o}.

Particle Image Velocimetry

The 2-D velocity vector distribution has been measured by digital particle image velocimetry (DPIV). By this method, the motion of the scattering particles, observed in the plane of the illuminating light sheet, are analysed. For this purpose, the colour images of TLC tracers are transformed to B&W intensity images. After applying special filtering techniques bright images of the tracers, well suited for DPIV, are obtained. Some additional experiments have been performed using colourless „classical" DPIV tracers (*pine pollen* or *lycopodium*).

The magnitude and direction of the velocity vectors are determined using a FFT-based cross-correlation analysis between small sections (interrogation windows) of one pair of images taken at the given time interval. The average particle displacement during a given time interval determines the velocity vector representing the section investigated. Through a moving (step by step) interrogation widow across the image, about 1000 vectors per one pair of images are obtained. The spatial resolution of the method is limited by the minimum amount of tracers present in the interrogation window. In practice, the minimum window size was 32x32 pixels. On the other hand, the dimension of the interrogation window limits the maximum detectable displacement. Hence, to improve the accuracy and dynamics of the velocity measurements short sequences of images have been taken at every time step. The cross-correlation analysis performed between different images of the sequence (time interval between pairs changes), allows us to preserve similar accuracy for both the low and high velocity flow regions.

For some experimental data, the newly developed ODP-PIV method (Quénot et al. 1998) of image analysis has been also used to obtain dense velocity fields of improved accuracy. In the cited paper results of several accuracy tests performed for the artificial images are given. It came out that for typical experimental conditions, i.e. images with 5% noise added and 5% particle disappearance, the accuracy of the „classical" FFT-based DPIV and that of the ODP-PIV method is 0.6 pixels and 0.15 pixels, respectively. It means that for typical displacement vector of 10 pixels the relative accuracy of the velocity measurement (for single point) is better than 6%.

To get a general view of the flow pattern, several images recorded periodically within a given time interval have been added in the computer memory. Displayed images are similar to the multiexposed photographs, showing the flow direction and its structure. This type of visualisation is very effective in detecting small re-circulation regions, usually difficult to identify in the velocity field. In all cases studied the volume concentration of tracers was very low (below 0.1%), so their effect on the flow and the physical properties of water was negligible small.

The flow images are used to evaluate shape and location of the phase front. These measurements are performed manually using image analysis software. The accuracy of single points measurement is about 1 pixel, what corresponds to 0.07 mm.

NUMERICAL MODEL

The obtained empirical results are further used to verify the performance and accuracy of the Finite Element model developed to simulate heat transfer and fluid flow in pure water solidification driven by heat conduction and buoyancy forces (Banaszek et al. 1997). The FEM algorithm is based on the semi-implicit operator splitting technique (Ramaswamy & Jue 1992) bind with the enthalpy-porosity approach (Brent & Voller 1988). Convection and diffusion are treated there separately, i.e.: convective terms of momentum and energy equations are integrated in time and space using the Taylor-Galerkin FEM, whereas diffusive terms are integrated by fully implicit scheme with the lumped heat capacity model.

Chorin's (1968) fractional step method is applied to decouple the continuity and momentum equations. First, the momentum equation with disregarded pressure gradient is solved and then the provisional velocity field, thus obtained, is corrected by taking into account the pressure contribution through the

enforcement of the incompressibility condition. In the temperature-range solidification of a binary system three different zones can be distinguished - namely, solid, liquid, and a mushy zone that consists of both these phases. At the liquid/solid interface the liquid velocity should take a zero value, whereas in the mushy zone it should gradually decrease with increase of the solid volume fraction. Such behaviour of the velocity field in the vicinity of a sharp or dispersed phase front is modelled by assuming that a mushy zone can be treated as a porous medium with porosity equal to the liquid volume fraction.

The pressure gradient is described by the Carman-Kozeny law (Ramaswamy & Jue 1992) and an additional source term is added to the momentum balance equation to imitate the above described behaviour of the system in the mushy zone. To solve a moving boundary phase change problem on a fixed FEM grid, Voller's source-based method (Voller & Swaminathan 1991) is generalised to calculate convective heat transfer effects.

SELECTED RESULTS

The empirical data have been collected for pure water and the water-salt solution to test the experimental methods and to obtain reference data for the flow properties.

Natural Convection

At the beginning, our interest was directed to understanding the transient behaviour of natural convection of water in the vicinity of the freezing point. The experiments start by abruptly dropping the cold wall temperature to 0^oC. The effects of density inversion and of the thermal boundary conditions at non-isothermal walls on the flow structures are studied to compare and eventually improve the numerical code.

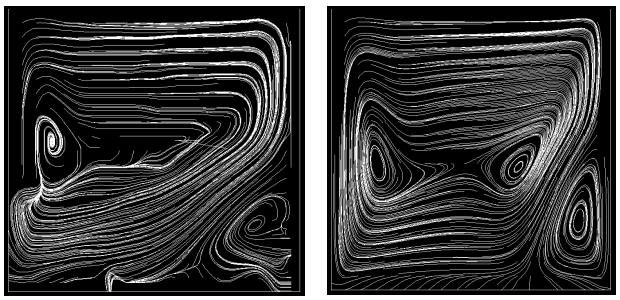

Fig. 3. Steady-state free convection of pure water, $T_c=0^oC$, $T_h=10^oC$. Streamlines calculated from DPIV experiment (left) and numerical simulation (right).

A typical flow structure exhibits two circulation regions *(Fig. 3a)*, where the water density decreases with temperature (upper) and an abnormal density variation (lower). It was found that the calculated flow pattern depends strongly on the modelling of the thermal boundary conditions at the side walls. Neither isothermal or constant heat flux models are sufficiently accurate to obtain observed flow structures. Solving the coupled solid-fluid heat conduction problem together with the Navier-Stokes equations improved modelling of the flow pattern (Fig. 3b).

The importance of the accurate description of the water density variation emerged, when several functions available in the literature were tested. Very small deviations in their functional form appeared to accomplish distinct changes in the flow structure. Hence, in further numerical simulations our fourth order polynomial fit to the tabulated data is selected as an optimal density function (Kowalewski & Rebow 1997).

Freezing of Water

The pure water freezing experiments show, as already mentioned, two main flow circulation regions. In the first, driven by „normal convection" and located in the upper part of the cavity, there is a clockwise circulation. It transports the hot liquid up to the top wall and back along the isotherm of the density extreme. Interaction of the hot liquid with the freezing front causes its melting and depletion of the freezing plane. The second flow circulation region, due to „abnormal convection", is located in the lower part of the cavity. There, a counter-clockwise circulation transports the cold liquid up along the adjacent ice surface and back to the bottom along the isotherm of the density extreme. This cold water circulation only moderately modifies the heat balance at the interface. The convective heat transfer between both upper and lower regions seems to be limited mainly to the upper right corner of the cavity. There, along the colliding cold and warm fluid layers, the heat is transferred from the hot wall to the lower parts of the cavity. The shape of the freezing front reproduces this interaction, almost doubling the ice growth rate at the bottom (comp. Fig. 4).

Most of the investigations concerning solidification assume the isothermal conditions at the phase change boundary and the temperatures above the freezing point for the liquid phase. However, it is well known that usually the fluid supercooling precedes the phase change. Our experiments with freezing water indicate that in most of the cases distilled water cools to about -7^oC before phase change begins. The observed effect of supercooling qualitatively changes the onset of freezing. Modelling of the supercooling for the ice formation was not present in the numerical model. Perhaps this is one of the reasons of the difficulties we encountered in achieving agreement between numerical and experimental data.

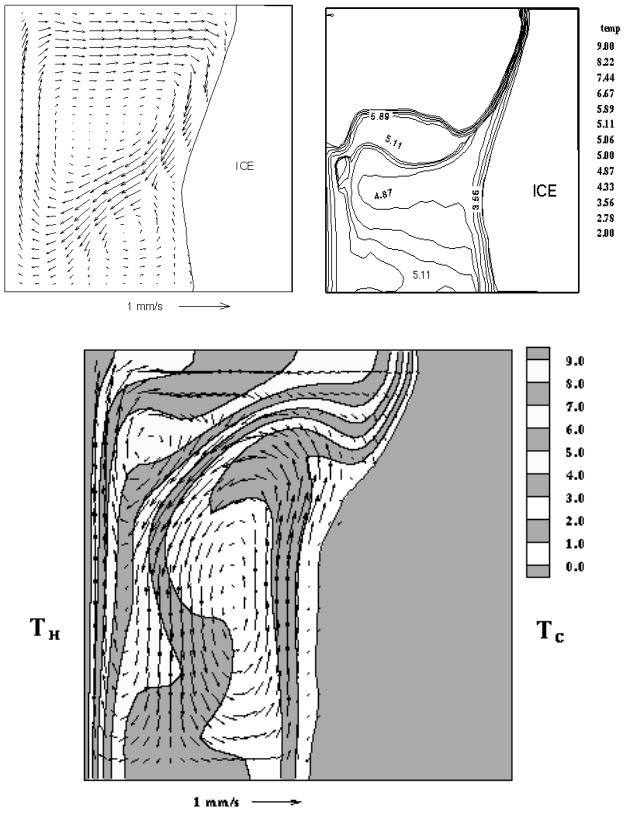

Fig. 4. Freezing of pure water, measured (upper row) and calculated (bottom) velocity and temperature fields at 2600s after cooling starts; $T_c= -10^oC$, $T_h= 10^oC$.

Freezing of Saline Solution

The thermohaline convection is studied for dilute aqueous solution of sodium chloride. The mass fraction of NaCl in the solution is 0.01. For this salinity temperature of the freezing point is equal -0.6°C, very close to that of water. The temperature of the density maximum decreases stronger with the salt concentration, and for our solution is equal 1.5°C. It is worth to note that temperature range, where the density anomaly plays a role, shrinks to about 2°C.

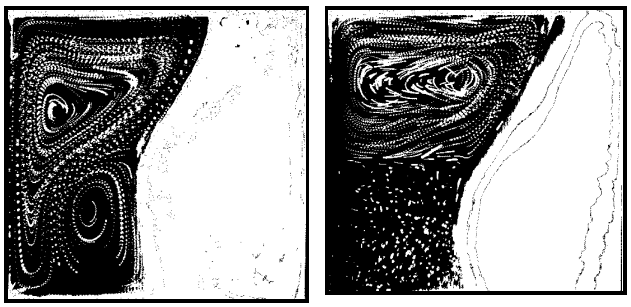

(a) (b)

Fig. 5. Ice front and particle tracks observed for pure water (a) and salt solution (b) at 3600 sec after cooling starts. Superposition of 10 images taken every 0.4s; T_c= -15°C, T_h= 10°C.

Before an experiment began the solution in the cavity was kept at a uniform temperature T_h=10°C, equal the hot wall and external bath temperatures. The experiment starts by allowing the refrigerant, pre-cooled to -15°C, to circulate through the „cold" wall antechamber. For comparison similar experiment is performed for pure distillated water filing the cavity.

The experiments performed for the water-salt solution indicate strong effects of the salt concentration on the „abnormal convection" structure. Even for a very small salt concentration, the observed flow pattern in the cavity changes completely, comparing with the pure water case (comp. Fig. 5).

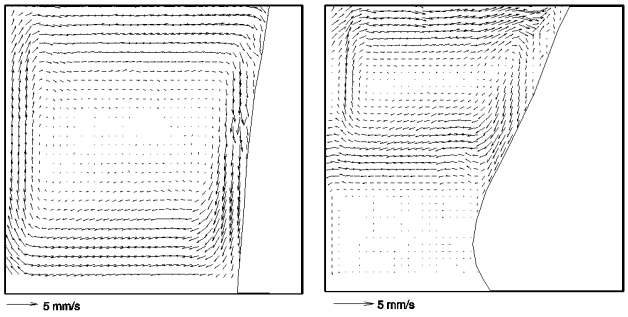

(a) t=500s (b) t=3000s

Fig. 6. Measured velocity fields for the salt solution at 500s (a) and 3000 s (c) after start of cooling; T_c= -15°C, T_h= 10°C.

For the salt solution only one regular circulation appears, which is typical for natural convection in a differentially heated cavity. Initially the main circulation extends to the whole cavity, with a clockwise circulation transporting the hot liquid to the solidus boundary. It appears, that the temperature range of the density anomaly is too narrow to generate the secondary circulation, and natural convection in this temperature range is completely dominated by the main flow. As the solid front propagates, the circulation flow region shrinks, both horizontally and vertically, moving its centre to the upper cavity area. Since dissolved salt is largely excluded in freezing, the salinity level will be higher nearer the interface. The heavier solution of higher salinity starts to accumulate at the cavity bottom. As the time passes the flow slows down, and small region of the secondary circulation appears above the mid-high of the ice surface (

Fig. *6*). The stagnant, bottom layer of higher salinity grows in time. There, due to the density gradient, the thermal effects become to weak to sustain convection, and after about 3000s the flow in the lower half of the cavity ceases practically completely. The upper regions characterise a double - roll convective pattern, typical for natural convection at medium Rayleigh numbers.

The temperature and velocity measurements confirm our general observation that the main fluid circulation takes place in the upper part of the cavity. There, the fluid temperature is relatively uniform, close to that of the hot liquid. The average flow velocity is almost one order of magnitude higher than in the bottom region. Also the largest temperature gradients occur in the lower cavity region.

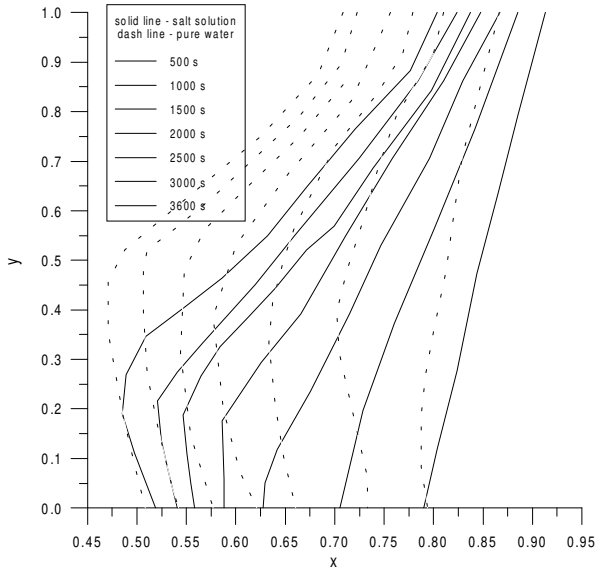

Fig. 7. Interface profiles measured for the pure water and the salt solution at selected time steps; T_c= -15°C, T_h= 10°C.

The front movement is appreciable affected by the flow. With the progressing ice interface, the lower circulation diminishes in time, whereas the upper one becomes stronger. The intense heat exchange slows down the ice growth in the upper part. Initially almost plane ice surface gets a characteristic "belly" in its lower part. There the heat transfer through the stagnant layer is mainly conduction controlled. After about 1 hour of the experimental observations less then one half of the cavity becomes frozen, with the strongly bowed interface.

Direct comparison of the measured progress of the solid-liquid interface for the pure water with the one for the salt solution for the same initial and boundary conditions shows several differences (*Fig. 7*). Generally, the interface for the pure water case moves faster than that for the salt solution. Also the largest growth of the ice takes place in the lower and mid part of the cavity. This is because for the pure water case the "hot" circulation spreads over smaller area. Hence, the heat flux from the hot wall reaches only upper corner of the freezing interface, before it is redirected back to the bottom along

the diagonal stream (Fig. 5a). Close to the bottom the growth rate of the interface is appreciable higher for the salt solution than for the pure water case. It takes almost 3000s before the positions of both interfaces overlapped there. It is due to the diminishing role of the secondary circulation for the pure water. Hence, in late phase of the experiments at the bottom the growth rate of the interface is controlled mainly by thermal conduction in both cases.

COMPARISONS AND DISCUSSION

Experimental data for freezing of water in the cube-shaped cavity have been gathered and interpreted for the purpose of creating a benchmark for comprehensive comparisons of the performance and accuracy of various numerical models for the challenging problem of buoyancy - driven solid-liquid phase change phenomena in both pure substances and binary mixtures.

The method of simultaneous measurements of the flow and temperature fields using liquid crystal tracers has been successfully applied to collect transient information on the flow. The obtained results show the complexity of the flow in the cases of a pure water and a water-salt solution. Two distinct flow regions are created due to the water density anomaly. The upper region adjacent to the hot wall has a strong clockwise convection of hot liquid, and a lower region adjacent to the interface has a slow counter-clockwise circulation of cold liquid. The mixing of both liquids seems to be small.

Hence, the effect of natural convection on the freezing process is mostly limited to the interface close to the top of the cavity. The heat flux through the Plexiglas bottom and top walls has relatively small significance for the freezing process.

Next, the empirical data have been used to verify the performance and accuracy of the FEM model developed. First, the free convection of water (without phase change), that does not obey the Boussinesq approximation, has been analysed and it has been found that the calculated solution agrees fairly well with the experimental findings (Fig. 3). However, in the more challenging case of freezing of pure water a visible incongruity in comparing the numerical solution and empirical data appears in the front shape and local flow pattern (Fig. 4). It seems that the model used overestimates the wall conduction.

Differences between numerical and experimental data can be explained by the limitation of the computational analysis to a two-dimensional flow approximation as well as by some freedom of definition of phase change region properties in the enthalpy-porosity approach. Moreover, such effects occurring in real freezing like supercooling, non-homogenous ice structure as well as non-ideal thermal contact between ice and the isothermal wall, are not included in the numerical analysis. Furthermore, it has been observed that the local flow pattern is very sensitive to the thermal boundary conditions at the upper and lower walls of the cavity. Our further efforts will be concentrated on more precise modelling of boundary conditions in the numerical model. Further numerical and experimental investigations seem to be necessary.

ACKNOWLEDGEMENTS

This work was supported by KBN (Polish Committee for Scientific Research), Grant No. 3T09C00212. Part of the computations were performed on CRAY-CS6400 at the Warsaw University of Technology (COI).

REFERENCES

Abegg, C., de Vahl Davis, G., Hiller, W.J., Koch, St., Kowalewski, T.A., Leonardi, E., Yeoh, G.H., 1994, Experimental and numerical study of three-dimensional natural convection and freezing in water; *Proc. of 10th Int. Heat Transfer Conf.*, Brighton, vol. **4**, pp. 1-6.

Banaszek, J., Rebow, M., Kowalewski T.A., 1997, Fixed grid finite element analysis of solidification, in *Adv. in Computational Heat Transfer*, CHT-97, .Begell House, New York (in press).

Brent A.D., Voller, V.R., 1988, Enthalpy-Porosity Technique for Modelling Convection-Diffusion Phase Change: Application to the Melting of a Pure Metal, *Numerical Heat Transfer,* vol. **13**, pp. 297-318.

Collins, M.W., 1991, Holographic techniques for whole-field thermal and fluid measurements, *Aeronautical J.,* vol. **95**, pp. 313-323.

Chorin, A.J., 1968, Numerical Solution of Navier-Stokes Equations, *Math. Comp*., vol. **22**, pp. 745-762.

Hiller, W.J., Koch, St., Kowalewski, T.A., 1988, Simultane Erfassung von Temperatur- und Geschwindigkeitsfeldern in einer thermischen Konvektionsströmung mit ungekapselten Flüssig-kristalltracern, in: *2D-Meßtechnik DGLR-Workshop*, Markdorf, DGLR-Bericht 88-04, pp. 31-39, DGLR Bonn.

Hiller, W.J., Koch, St., Kowalewski, T.A. & Stella, F., 1993, Onset of natural convection in a cube, *Int. J. Heat Mass Transfer*, vol. **36**, pp. 3251-3263.

Hiller, W., Kowalewski, T.A., 1987, Simultaneous measurement of the temperature and velocity fields in thermal convective flows, in *Flow Visualisation IV, Paris 1996*, Ed. Claude Veret, pp. 617-622, Hemisphere, Paris.

Kowalewski, T. A. Cybulski A., 1996, Experimental and numerical investigations of natural convection in freezing water, *Int. Conf. on Heat Transfer with Change of Phase*, Kielce, in Mechanics, vol. **61**/2, pp. 7-16.

Kowalewski T.A., Rebow M., 1997, An experimental benchmark for freezing water in the cubic cavity, in *Adv. in Computational Heat Transfer*, CHT-97, .Begell House, New York (in press).

Quénot G., Pakleza J., Kowalewski T.A., 1998, Particle Image Velocimetry with Optical Flow, *Experiments in Fluids*, to appear.

Ramaswamy, B., Jue, T.C., 1992, Some recent trends and developments in finite element analysis for incompressible thermal flows, *Int. J. Num. Meth.. Eng.,* vol. **35**, pp. 675-692.

Stąsiek J., Collins M., 1989, Design of wind tunnel and review of liquid crystal thermography, Report for PowGen., Thermo-Fluids Eng. Res. Centre, City University.

Voller, V.,R., Swaminathan, C.,R., 1991, General source-based method for solidification phase change, *Numerical Heat Transfer*, Part B, vol. **19**, pp.175-189.

Examples of colour images of the flow field can be found at our WWW server: http://www.ippt.gov.pl/~tkowale/